J Neurophysiol 117: 2025–2036, 2017.
First published February 22, 2017; doi:10.1152/jn.00546.2016.

RESEARCH ARTICLE | *Control of Movement*

Multidigit force control during unconstrained grasping in response to object perturbations

Abdeldjallil Naceri,[1] Alessandro Moscatelli,[2,3] Robert Haschke,[1] Helge Ritter,[1] Marco Santello,[4] and Marc O. Ernst[5]

[1]*Neuroinformatics Group, Cluster of Excellence Cognitive Interaction Technology (CITEC), Bielefeld University, Bielefeld, Germany;* [2]*Department of Systems Medicine and Centre of Space Bio-medicine, University of Rome "Tor Vergata," Rome, Italy;* [3]*Laboratory of Neuromotor Physiology, IRCCS Santa Lucia Foundation, Rome, Italy;* [4]*School of Biological and Health Systems Engineering, Arizona State University, Tempe, Arizona; and* [5]*Faculty for Computer Science, Engineering, and Psychology, Ulm University, Ulm, Germany*

Submitted 11 July 2016; accepted in final form 18 February 2017

Naceri A, Moscatelli A, Haschke R, Ritter H, Santello M, Ernst MO. Multidigit force control during unconstrained grasping in response to object perturbations. *J Neurophysiol* 117: 2025–2036, 2017. First published February 22, 2017; doi:10.1152/jn.00546.2016.—Because of the complex anatomy of the human hand, in the absence of external constraints, a large number of postures and force combinations can be used to attain a stable grasp. Motor synergies provide a viable strategy to solve this problem of motor redundancy. In this study, we exploited the technical advantages of an innovative sensorized object to study unconstrained hand grasping within the theoretical framework of motor synergies. Participants were required to grasp, lift, and hold the sensorized object. During the holding phase, we repetitively applied external disturbance forces and torques and recorded the spatiotemporal distribution of grip forces produced by each digit. We found that the time to reach the maximum grip force during each perturbation was roughly equal across fingers, consistent with a synchronous, synergistic stiffening across digits. We further evaluated this hypothesis by comparing the force distribution of human grasping vs. robotic grasping, where the control strategy was set by the experimenter. We controlled the global hand stiffness of the robotic hand and found that this control algorithm produced a force pattern qualitatively similar to human grasping performance. Our results suggest that the nervous system uses a default whole hand synergistic control to maintain a stable grasp regardless of the number of digits involved in the task, their position on the objects, and the type and frequency of external perturbations.

NEW & NOTEWORTHY We studied hand grasping using a sensorized object allowing unconstrained finger placement. During object perturbation, the time to reach the peak force was roughly equal across fingers, consistently with a synergistic stiffening across fingers. Force distribution of a robotic grasping hand, where the control algorithm is based on global hand stiffness, was qualitatively similar to human grasping. This suggests that the central nervous system uses a default whole hand synergistic control to maintain a stable grasp.

control; force; grasping; manipulation; unconstrained

WHENEVER WE GRASP and lift an object, our sensorimotor system is faced with the challenging task of precisely controlling the multiple degrees of freedom of the hand, such as joints and muscles to counteract the interaction forces and torques. Additionally, the sensorimotor system has to take into account the object's properties, such as its shape, estimated weight, center of mass, friction coefficient, and the goal of the planned action to achieve grasp stability (Fu et al. 2010; Lukos et al. 2007, 2008). The control of finger forces in grasping and manipulation tasks requires a combination of sensorimotor predictions and feedbacks from the somatosensory and the visual system (Johansson and Flanagan 2008; Johansson and Westling 1984; Westling and Johansson 1984). Specifically, a feedforward mechanism is engaged on the basis of predictions derived from internal representations of the hand and the object. The feedback mechanism is engaged at late grasping stage when prediction error arises, thus generating corrective responses and updating the internal representations of object properties (Johansson and Flanagan 2008). Finally, controlling the muscle activation threshold has also been proposed as an alternative mechanism, i.e., the muscle length at which motor neurons begin their recruitment (Latash et al. 2010; Pilon and Feldman 2006; Pilon et al. 2007).

Because of the many degrees of freedom of the human hand, a given object can be grasped successfully in many different ways and with virtually an infinite number of distinct postures. Therefore, the central nervous system (CNS) has to master this redundancy in the number of degrees of freedom to make the most appropriate choice of digit contact points with the object and modulation of grip, load forces, and torques across the fingers (Friedman and Flash 2007; Russo et al. 2014).

Synergies are defined as a functional property of the sensorimotor system where a specific group of joints and muscles are constrained to act as single units working toward a specific motor goal (Santello et al. 2013, 2016). Hence, synergies could provide a viable strategy to solve the problem of motor redundancy (Latash 2012; Santello et al. 1998, 2013). In this study, we exploited the technical advantages of an innovative sensorized object to study unconstrained hand grasping within the theoretical framework of motor synergies. In each trial, partic-

Address for reprint requests and other correspondence: A. Naceri, Neuroinformatics Group, Cluster of Excellence Cognitive Interaction Technology (CITEC), Bielefeld University, 33619 Bielefeld, Germany (e-mail: abdeldjallil.naceri@uni-bielefeld.de).

ipants were required to grasp, lift, and hold the sensorized object. The design of the sensorized object was such that in each trial, participants could freely choose the location of the digits on the object. During the holding phase, we repeatedly applied external disturbance forces and torques. We recorded the temporal and the spatial distribution of grip forces produced by each digit.

The current study had three aims. First, we investigated the existence of idiosyncratic hand posture characterizing different individual participants. To achieve grasp stability, the sensorimotor system controls each digit's placements and forces to counteract the external torques and forces produced by gravity and occasional perturbations (Baud-Bovy and Soechting 2002; Friedman and Flash 2007; Fu et al. 2010; Naceri et al. 2014). In most previous studies, the position of the digits on the grasped object was constrained due to technical limitations of the experimental devices. In Fu et al. (2010), the authors compared a constrained and an unconstrained two-digit grasp (pinch grasping) and showed that the adoption of a noncollinear digit placement in unconstrained grasping allowed participants to optimize the grip forces. The authors reported trial-to-trial variability in initial digit placements during unconstrained grasping, as well as variability in force modulation to digit placement to ensure the attainment of the target torque. However, it is still largely unknown how participants control digit placements in more complex grasping tasks that involve more than two digits. We addressed this question by running a cluster analysis on digit positions of individual participants.

The second aim was to evaluate whether participants controlled independently each individual digit or, conversely, adjusted the stiffness or force of the whole grasp, consistent with the hypothesis of a synergistic hand control (Santello et al. 2013, 2016). To address this scientific question, we delivered a variety of force and torque perturbations to systematically assess the extent to which the distribution of force response across digits would reflect specific perturbations. Alternatively, participants could increase the global stiffening of the whole hand, irrespective of the perturbation types. Previous studies on constrained multidigit grasping suggested that the CNS controls separately the normal force of each individual digit depending on the external mechanical perturbations (Wu et al. 2012; Zatsiorsky and Latash 2004; Zatsiorsky et al. 2002). Specifically, the index and the little fingers would play a crucial role to counteract an external torque perturbation, whereas the middle and the ring fingers would produce most of the load force required for grasp stability. This hypothesis is referred to as "finger specialization" (Wu et al. 2012; Zatsiorsky et al. 2002). In contrast, other studies based on electromyographic recordings concluded that the CNS controls the global hand stiffness rather than the grip force in individual digits in tripod grasp (Winges et al. 2007). The authors observed a force tuning at the levels of the individual digits, but the maximum grip force tended to remain the same across conditions, consistently with the hypothesis of a global hand stiffness control (Winges et al. 2007).

In the current study, we analyzed the temporal distribution of peak force exerted by each digit and cross-correlation of digit force profiles in response to external perturbations to determine whether force responses across multiple digits are synchronous. This would support the hypothesis of a synergistic control of the hand, regardless of the grasp configuration and perturbations (Winges et al. 2007). Conversely, a broad distribution of digit peak forces and low cross-correlation coefficients between force profiles would suggest an independent control of the different digits. We further evaluated the issue of independent control of the individual digits by comparing the force distribution of human grasping vs. robotic grasping, where the control strategy was set by the experimenter. We controlled the global hand stiffness of the robotic hand but not the force exerted by each digit, and we tested whether this control algorithm produced a force pattern comparable with human grasping performance.

Finally, our third aim was to address whether participants adjusted forces across digits during the holding phase on the basis of sensory feedback from proprioception and touch (closed loop) or predictive mechanisms (feedforward). We hypothesized that the CNS would utilize a feedforward control of multiple digit forces within a single perturbation and across perturbations, in accordance with Budgeon et al. (2008). To test our hypothesis, we delivered force and torque perturbations within time intervals that were either predictable (periodic) or unpredictable (aperiodic) while participants were instructed to hold the object stationary. If the hypothesis of the feedforward control were true, participants should adopt a similar motor strategy regardless the number of digits involved in the grasping task, perturbation type, and perturbation frequency.

METHODS

Participants. Twenty-one right-handed participants (8 women, 24 ± 6 yr of age) took part in the experiment. Five participants participated in the two-digit condition, five participated in the three-digit condition, five participated in the four-digit condition, and six participated in the five-digit condition. All participants had no history of neurological or motor deficits. The testing procedures were approved by the ethics committee of Bielefeld University, in accordance with the guidelines of the Declaration of Helsinki for research involving human participants. Informed written consent was obtained from all participants involved in the study.

Experimental setup. The experimental device, referred to as the tactile object (TACO), records the position and the normal force exerted by each finger on its sensorized surface and facilitates participants freely choosing digit positions on the object for unconstrained grasping. The TACO has a cuboid shape (length, $l = 170$ mm; height, $h = 85$ mm; width, $w = 55$ mm). Four high-speed tactile sensor modules (Schurmann et al. 2011), subsequently named "Myrmex," are mounted on two opposing faces of the cuboid. Each Myrmex module provides a 16×16 tactile array on an area of 80×80 mm^2 and has a sampling rate of up to 1.9 kHz and spatial resolution of 5 mm (one sensor element). The TACO consists of four Myrmex (1,024 tactels) modules mounted on both the front and back surface plane, two on the front and the other two on the back (Schurmann et al. 2012). The TACO allows us to simultaneously record the center of pressure and the normal force exerted by each digit. The device is calibrated using a force gauge with a force ranging from 0 to 25 N. During the calibration, we varied the cross-sectional area of the gauge tip from 10 to 50 mm^2 with a step of 20 mm^2 to account for differences in fingertip size between participants.

A mirrored screen occluded the participants' hands and the TACO from sight, removing any visual feedback of their hand location and grasp. The mirror faced a computer monitor (21-in. CRT, SONY CPDG520, with a resolution of $1,280 \times 1,024$ pixels and refresh rate of 100 Hz) that we used to display the visual stimulus. The visual stimulus consisted of a rectangular cuboid, with the same dimensions

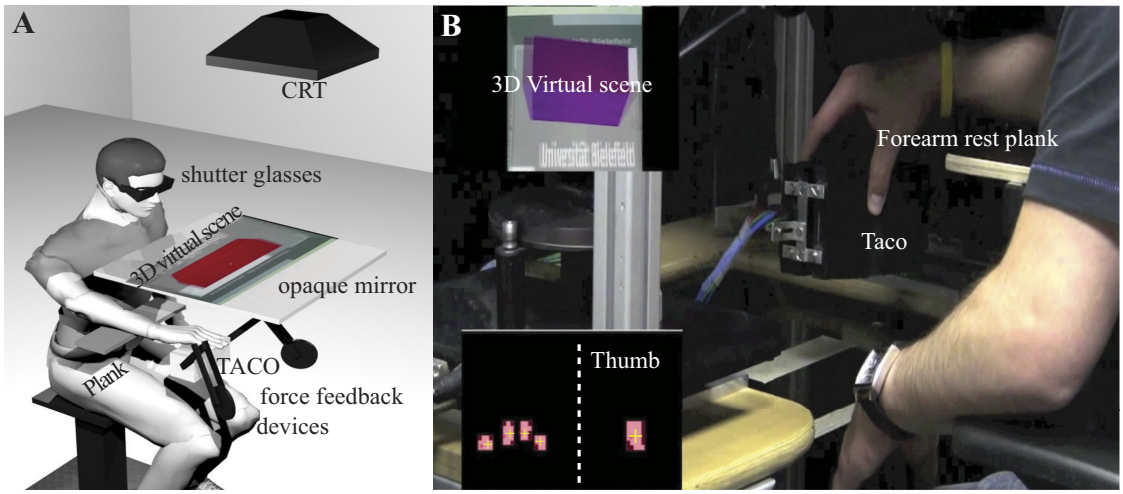

Fig. 1. Experimental setup. *A*: participants binocularly viewed the mirror image of the visual scene. *B*: the TACO attached to the PHANToM force feedback devices. *Top left*, 3-D virtual scene, where the purple cube color indicates to participants the desired height (red color otherwise, as shown in *A*). *Bottom left*, TACO output image, where a yellow cross represents digit centers of pressure (CoPs).

of the TACO. Participants wore liquid-crystal shutter glasses (CrystalEyes) providing binocular disparity (Fig. 1*A*).

The TACO was attached to two PHANToM (SensAble Technologies) force-feedback devices to track its position and allow force/torque perturbations to be applied during the holding phase of the trial (Fig. 1*B*). The sampling rate of the PHANToM is 1 kHz, allowing a precise position match between the simulation and the TACO. The total mass of TACO is 0.470 kg. Because of the constraints of the two PHANToM devices, the TACO has five degrees of freedom: translation along the x, y, and z directions, and rotation along the yaw (α) and roll (β) axes (Fig. 2*A*).

In the control experiment, we replicated the task using the Shadow Dexterous Hand (Shadow Robot Company, London, UK), which is a humanoid robotic hand endowed with approximately the same kinematics and number of degrees of freedom as the human hand (Fig. 3*A*). The hand has 18 actively controlled degrees of freedom (DoF) plus 2 DoF for the wrist (abduction/adduction and flexion/extension). Movements of the Shadow Dexterous Hand closely resemble those of a regular human participant (Rothling et al. 2007). An antagonistic pair of McKibben-style pneumatic muscles actuates each joint in an inherently compliant fashion, thus mimicking human muscle properties. We employed a stiffness control of the artificial muscles. The stiffness was fixed during each grasping trial. The maximum normal force produced by each finger opposing the thumb during object perturbation was ~8 N. The Shadow Dexterous Hand was attached to a KUKA lightweight robot4+ "KUKA-LWR4+" as the end effector (Fig. 3*B*) to mimic the lifting movements of the TACO performed by human participants.

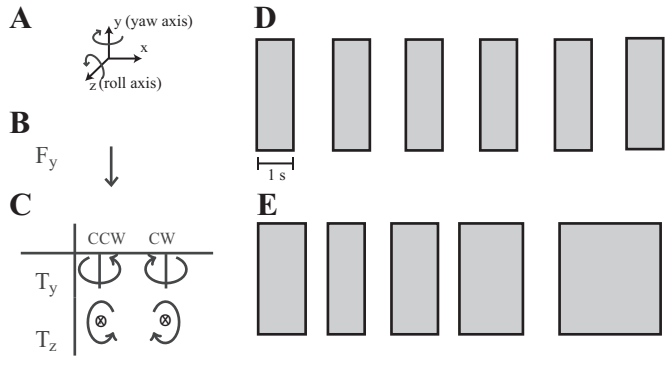

Fig. 2. Experimental protocol. *A*: world frame of reference. *B*: perturbation force F_y (downward). *C*: perturbation torques T_y and T_z clockwise (CW; T_y^{CW} and T_z^{CW}) and counterclockwise (CCW; T_y^{CCW} and T_z^{CCW}). *D* and *E*: examples of periodic (P) and aperiodic (Ap) trials, respectively. Gray-shaded boxes represent intervals when force/torque perturbations are applied.

Procedures. Participants sat on a chair with an adjustable height. Before the start of the grasping movement, participants' forearms rested on a plank with the palm of the hand facing downward. Participants received an auditory "GO" signal, instructing them to grasp the TACO and to lift it to a target height of 100–150 mm. A simulated rectangular cuboid was displayed on the CRT via the mirror with the appropriate size and in the same location as the TACO. Upon lifting, the virtual representation of the TACO changed color to inform participants that the TACO had reached the desired target height. At that height, participants were asked to hold the TACO as still as possible, irrespective of any disturbance forces acting on the object. After having stabilized the TACO for ~20 s, participants received another auditory signal cueing them to place the TACO back on the table. In different experiments participants were instructed to grasp the TACO with two, three, four, or five fingers (thumb-index finger, thumb-index-middle fingers, thumb-index-middle-ring fingers, or all fingers of one hand). Fingers not involved in the task were extended and taped to a splint made of cardboard to prevent them from contacting the TACO. The finger placements on the TACO were self-chosen (grasping without constraints).

During the object holding phase, perturbation forces and torques were applied using the PHANToM force-feedback devices. We evaluated five force/torque conditions (perturbation type) and two periodical/aperiodical perturbations (perturbation frequency). In the F_y condition, a force of 2.4 N was applied along the vertical direction (downward; Fig. 2*B*). In the T_y and T_z conditions, torques of 0.25 N·m were applied around the y- or z-axis (Fig. 2*C*), causing respectively yaw and roll rotations around the TACO's center of mass. Perturbation torques, T_y and T_z, were applied in clockwise (CW) and counterclockwise (CCW) directions. In one instance the applied force and torques were turned "on" and "off" periodically (perturbation frequency) and were thus "predictable" in terms of frequency and timing (Fig. 2*D*). In the other instance, the applied perturbation forces and torques occurred aperiodically. That is, the onset times for the perturbations "on" ranged at random between 1 and 3.5 s after the last offset of the perturbation and had a random duration between 0.6 and 1 s. They were thus "unpredictable" (Fig. 2*E*). The rationale of this experimental design was to test whether the grasping forces of the fingers would depend on the predictability of the perturbations and therefore adapt differently to the two temporal patterns of the perturbations. Overall, there were $5 \times 2 = 10$ conditions: 5 force pertur-

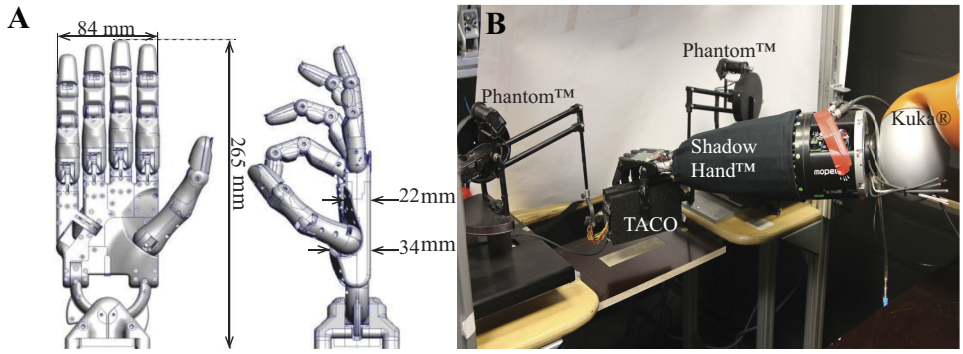

Fig. 3. The Shadow Dexterous Hand. *A*: kinematics and degrees of freedom. *B*: the Shadow Dexterous Hand grasping the TACO attached to the KUKA light-weight robot4+ end effector.

bations types, F_y, T_y^{CCW}, T_y^{CW}, T_z^{CCW}, and T_z^{CW}, applied either periodically or aperiodically (the two perturbation frequencies, P and Ap). The order of conditions was randomly presented to the participants. Participants performed 10 trials per condition. Each trial lasted ~25 s from grasp onset to release. Before starting the experiment, participants were informed that during the holding phase the two PHANToM devices would apply periodic or aperiodic perturbations to the TACO and that the perturbation type would remain the same within each trial. Before the experiment, participants performed four trials with F_y perturbation applied periodically to familiarize themselves with the task. The total duration of the experiment was ~2 h per participant with a few minutes' break at the halfway point. Participants were also allowed to take a short break and rest at the end of each trial whenever they wanted.

In the control experiment, we replicated the same task performed by human participants (5-fingers condition) using a robotic hand (Shadow Dexterous Hand) in combination with the TACO. The hand controller developed by Rothling et al. (2007) is based on two control variables: joint position and joint stiffness. Each joint is controlled by a pair of air pressure-controlled artificial muscles. Whereas the difference in pressure correlates with the joint position, the pressure sum correlates to the joint's stiffness. The passive compliance of the muscles physically realizes an impedance control whose stiffness is adjustable. In this experiment, we chose a fixed stiffness of the grasping posture that allowed successful grasping and lifting of the TACO. The successful grasping posture of the robot hand was saved (referred to as "grasp" later in the text) and used during the whole experiment (the same posture across trials). Thus the hand had two states: release state, in which the hand was fully opened and there was "no grasp," and grasp state, in which the "grasp" posture was applied and the TACO was grasped. The positions of the robotic finger during the "grasp" posture would result in complete closure of the hand if applied in free space. The presence of the object, however, prevents the fingers from complete closure and ensures grasp forces are applied passively due to the inherent compliance of the hand when the TACO is present (Rothling et al. 2007). After the GO signal, the Shadow Dexterous Hand grasp state was changed from "no grasp" to "grasp." Once the hand successfully grasped the TACO (Fig. 3*B*), the experimenter lifted the TACO using KUKA-LWR4+. When the arm reached the intended height, the KUKA-LWR4+ was grounded to avoid any oscillations due to active control that could have altered the grasp performance. During the object hold phase, the PHANToM applied either T_y^{CCW} or T_y^{CW} perturbation (Fig. 2*C*) in a periodic or aperiodic fashion. We used only these two perturbations because of the low friction forces between the Shadow Dexterous Hand and the TACO. At the end of each trial, the KUKA-LWR4+ placed the TACO back on the table and the hand grasp state was set to "no grasp," releasing the TACO. Each perturbation was repeated 16 times, giving a total of 64 trials.

Crucially, the robot hand was not programmed to actively control grasping forces of individual digits to counteract the disturbances. Instead, the stiffness was fixed during each grasping trial, and the passive compliance of the artificial muscles resembles the mechanical properties of the muscles of the human hand and forearm. Hence, the robotic hand provides a plausible model for a grasping strategy based on the control of the global hand stiffness, as suggested (Winges et al. 2007).

Data processing. The normal forces (F) of the fingers and their positions, derived as the digit horizontal and vertical center of pressures (CoP_x and CoP_y), respectively, were read from of the TACO. We set the center of the TACO as the origin of the coordinate system (0, 0, 0). CoP_x and CoP_y were defined as the location of the global maximum of the activated region of tactels for each finger's region in the output matrix. The output matrix was converted to Newtons using the lookup table generated during calibration. The calibration table was obtained with a resolution of ±0.2 N. Digit locations, normal forces, and TACO position were recorded and processed with a second-order Butterworth low-pass filter with 10-Hz cutoff frequency (Fig. 4). The CoP_x and CoP_y values used for further analysis were extracted during the holding phase.

The three-dimensional (3-D) position and the rotations around the yaw and roll axes of the TACO were tracked using the PHANToM devices. They were further used to compute the net torques generated by the participant (HT_y, HT_z) using Newton's second law for rotation:

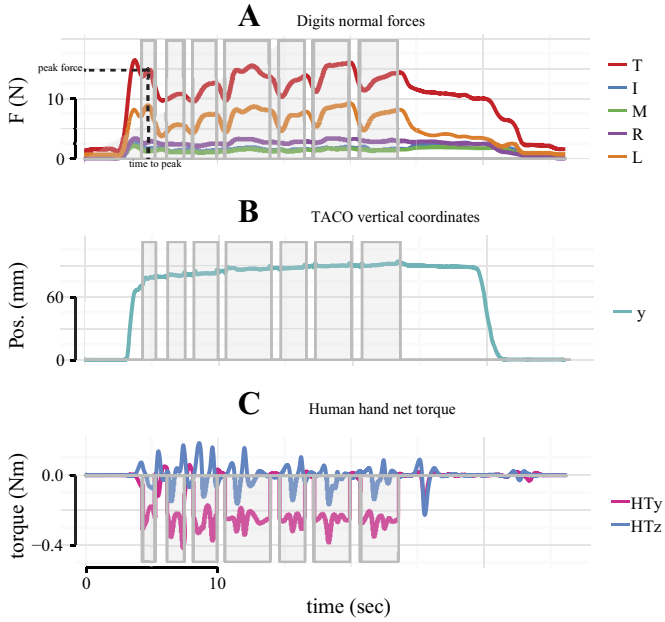

Fig. 4. Single trial of a representative participant (5 digits, T_y^{CCW}, perturbation applied aperiodically; digits indicated by color coding; areas boxed in gray represent 1 example of aperiodic intervals when external perturbations are active "on"). *A*: force profiles for each digit. *B*: TACO vertical coordinates along *y*-axis. Pos., position. *C*: participant's hand net torques (HT_y, HT_z).

$$\begin{cases} HT_y + T_y = \dfrac{d^2\alpha}{dt^2} I_y \\ HT_z + T_z = \dfrac{d^2\beta}{dt^2} I_z \end{cases} \quad (1)$$

where T_y and T_z are external torques, $d^2\alpha/dt^2$ and $d^2\beta/dt^2$ are the angular accelerations, and I_y and I_z are approximated to rectangular cuboid moments of inertia:

$$\begin{cases} I_y = \dfrac{1}{12} m\left(l^2 + w^2\right) \\ I_z = \dfrac{1}{12} m\left(l^2 + h^2\right) \end{cases} \quad (2)$$

The parameters m, l, w, and h correspond to the mass of the TACO attached to the arms of the PHANToM device and its length, width, and height, respectively.

To satisfy a stable grasp of the TACO, the force produced by the thumb must be equal to the sum of opposing digit normal forces:

$$\Sigma F_i^n = 0, \quad i = \text{T, I, M, R, L} \quad (3)$$

where T is the thumb and I, M, R, and L are the index, middle, ring, and little fingers, respectively. The two PHANToM devices did not support the weight of TACO. Hence, the sum of digits' load force must equal to the TACO load force:

$$\Sigma F_i^t = -mg, \quad i = \text{T, I, M, R, L} \quad (4)$$

where m is the TACO's mass and g is the gravity. Finally, load force is a function of grip force and friction coefficient (μ). Hence, this third constraint holds:

$$F_i^t < \mu F_i^n \quad (5)$$

Statistical analysis. First, we evaluated whether digit positions on the TACO were idiosyncratic, that is, whether there was a consistent pattern within each participant. To this end, we computed for each participant and condition the mean CoP_x and CoP_y of the different digits, averaged across trials and perturbation type. The averaged data are plotted in Fig. 5. These data were used to conduct a cluster analysis on the CoP_x and CoP_y of the fingers opposing the thumb in the three-, four-, and five-finger conditions. We did not include the thumb in the analysis because it contacted the opposite face of the TACO; i.e., it was projected on a different plane in the CoP space. We used *k*-means clustering: in the different conditions, we set the number of clusters to $k = 2$, 3, or 4 corresponding to the 2, 3, or 4 fingers opposing the thumb. The analysis aimed at investigating whether the initial placement of the different fingers was preserved within each participant and across perturbation type, that is, whether the hand posture was "idiosyncratic." Furthermore, we ran two-way ANOVA on the mean CoPs (factors: digit and participant) to test whether hand posture was significantly different between participants. We tested the cluster mean CoP_x and CoP_y separately.

In each perturbation number and for each digit we computed the time to reach the maximum grip force (time to peak). If the maximum force were to occur approximately at the same time between different digits, it would suggest a parallel control of digits to stabilize the object. To test this hypothesis, we used a multivariable linear mixed models (LMM) analysis evaluating whether the time to peak varied systematically across different digits. The time to peak (measurement variable denoted by "**y**" in *Eq. 6*) was modeled as a linear combination of the experimental variables (referred to as the fixed-effect linear predictors, $\boldsymbol{X\beta}$), the random variability between participants (the random-effect predictors, $\boldsymbol{Zb}$), and the residual random error, $\boldsymbol{\varepsilon}$ (Bates et al. 2015).

The LMM equation has the following general form:

$$y = X\beta + Zb + \varepsilon \quad (6)$$

The matrix of fixed-effect predictors, $\boldsymbol{X}$, included the following dummy-coded predictors: digit (T and, depending on the condition, I, M, R, L), perturbation number (P1, P2, P3, P4, P5), perturbations types (F_y, T_y^{CCW}, T_y^{CW}, T_z^{CCW}, and T_z^{CW}), and frequency (P, Ap). We considered only the first five perturbations in the analysis to have an equal number of stimuli in the periodic and aperiodic conditions. To obtain a balanced design, we fit the model separately for the two-, three-, four-, and five-digit conditions. We evaluated the effect of each digit by testing the significance of the corresponding fixed-effect

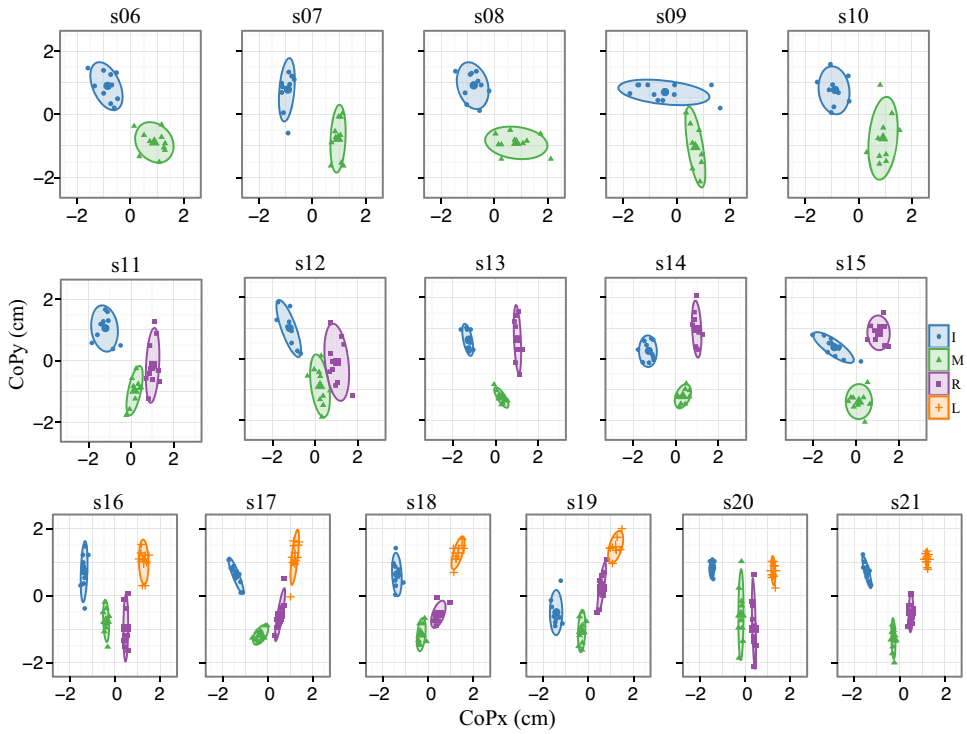

Fig. 5. Spatial distribution of horizontal (CoP_x) and vertical centers of pressure (CoP_y) of different digits (thumb not included). Each panel represents data from an individual participant, averaged across trials (10 points per participant per digit, corresponding to 10 perturbation conditions). Data are from 3-, 4-, and 5-digit conditions. Ellipsoids with shaded area represent cluster analysis results using *k*-means method on CoP data points without the thumb data. K-means method clustered the original data points correctly for each digit with the only exception being M and R digits in *participant s12*, whose positions were partially overlapping.

parameter β_{digit} with the likelihood ratio (LR) test (Pinheiro and Bates 2000). The LR test compares the maximized log-likelihood functions of two nested models, M1 and M0, with and without the parameter of interest, respectively. Under the null hypothesis that the simpler model, M0, is better than M1, the LR has a large-sample χ^2_1 distribution (Bolker et al. 2009; Moscatelli et al. 2012). We confirmed the results using a repeated-measures ANOVA.

Next, we studied the effect of learning and adaptation to the perturbations in each trial. To this end, we evaluated whether the value of peak force (in N) and the error in hand net torque changed with the number of perturbations within a trial. We fit a polynomial LMM including the following fixed effect predictors: perturbation number (P1, P2, P3, P4, P5), digit (T and, depending on the condition, I, M, R, L), perturbation type (F_y, T_y^{CCW}, T_y^{CW}, T_z^{CCW}, and T_z^{CW}), and frequency (P, Ap). To account for nonlinear effect, we used a second-order polynomial of the form $\beta_1 P + \beta_2 P^2$ for fitting, where P is the perturbation number and $\beta_{\{1,2\}}$ are the fixed-effect parameters. We evaluated the significance of the effect using the LR test.

To evaluate the contribution of each finger to the task, we studied the variation of normal force between the different fingers. We averaged data from each participant across the five perturbation numbers and across the periodic and aperiodic conditions. Within each trial, we subtracted the mean value of normal force of the index finger from the normal force of each other finger [F(diff) = F(M or R or L finger) – F(I finger)]. This aimed to compare the force change between fingers across different experimental conditions (3-, 4- and 5-digit grasp) that were collected on different participants (i.e., see Fig. 10). Using LMM, in torque perturbations we evaluated the modulation of actual normal force for digit and torque direction. We ran the analysis separately for each torque direction; therefore, it was not necessary to subtract the force value of the index finger as we did for the plot of Fig. 10. We applied the LR test to evaluate whether the difference in normal force between digits and torque direction was statistically significant. We did not include the two-digit condition in the analysis or in Fig. 10 because the thumb and the index digits share equally the total grip force.

We replicated the experiment using the robotic Shadow Dexterous Hand to evaluate whether the passive stiffness control of the robot would reproduce a similar pattern of forces as did the human participants. For the comparison, we computed the same measurements for the robotic hand as we did for human participants: the digit normal forces, the time to peak force, and the error in hand net torques. We modeled the data with the robotic hand using a simple linear model. The data from the robotic hand were not clustered like the human data, which include multiple participants. Hence, it was not necessary to use mixed models for this analysis.

RESULTS

In previous studies that investigated three-, four- and five-digit grasping (Baud-Bovy and Soechting 2002; Zatsiorsky and Latash 2008), digit position was highly constrained. Because of the custom-developed sensorized object used in this study, participants could perform a completely unconstrained multidigit grasp. We evaluated whether each participant used a stereotyped hand posture across different perturbation types, hence a characteristic pattern of digit position, as follows. Within each participant and digit condition, we averaged CoP_x and CoP_y across the different trials (resulting in 10 points per participant, corresponding to 10 perturbation conditions). Average CoP_x and CoP_y values are plotted in Fig. 5 for each participant.

Figure 5 shows the results of the *k*-means cluster analysis. The thumb was not included in the analysis because it touched the object on the opposite side of the cuboid, and hence its CoP was constrained on a different plane with respect to the other fingers. The cluster analysis correctly classified the different digits (Fig. 5) with one exception, which were the middle and ring fingers of *participant s12*, whose positions were partially overlapping. Within each participant, the relative position of each digit was approximately preserved across stimulus repetitions, consistent with an idiosyncratic distribution of digit position. In addition, we ran two-way ANOVAs on the mean CoP values (factors: digit and participant) to test whether hand posture was significantly different across participants. We separately tested CoP_x and CoP_y in the three-, four-, and five-digit conditions. The factor "participant" was always statistically significant for all digit conditions, in both *x* and *y* directions ($P < 0.001$ except in 3-digit condition/CoP_x $P = 0.03$). The factor "digit" was always statistically significant ($P < 0.001$). Taken together, cluster analysis and two-way ANOVA support the hypothesis of an idiosyncratic grasping posture. Overall, the finding of an idiosyncratic or "natural" hand posture provides a supporting argument for our ecological method of allowing for unconstrained grasping to investigate natural grasping behavior.

We used LMM to test whether the time to reach the maximum force (time to peak) was significantly different between the digits. As shown in Table 1, the estimated difference in time to peak force between the digits in any digit number condition was in the order of tens of milliseconds. Figure 6

Table 1. *LMM estimates for mean time to peak for each digit in periodic and aperiodic perturbation conditions and in 2- to 5-digit conditions*

	Thumb	Index	Middle	Ring	Little
2 Digits					
Periodic	221 [144, 305]	221 [148, 301]	NA	NA	NA
Aperiodic	1,229 [1,062, 1,396]	1,229 [1,053, 1,404]	NA	NA	NA
3 Digits					
Periodic	216 [133, 288]	222 [150, 288]	232 [157, 299]	NA	NA
Aperiodic	1,120 [988, 1,289]	1,100 [940, 1,245]	1,100 [931, 1,240]	NA	NA
4 Digits					
Periodic	465 [287, 521]	497 [327, 492]	456 [302, 503]	462 [292, 463]	NA
Aperiodic	1,230 [1,027, 1,311]	1,170 [942, 1,216]	1,180 [969, 1,259]	1,185 [944, 1,231]	NA
5 Digits					
Periodic	476 [411, 551]	443 [381, 518]	448 [390, 523]	449 [383, 521]	487 [466, 560]
Aperiodic	1,254 [1,120, 1,399]	1,247 [1,121, 1,381]	1,257 [1,119, 1,388]	1,207 [1,074, 1,336]	1,206 [1,092, 1,357]

Values are estimates of time to peak (in ms) computed as the difference between the onset of the perturbation and peak force. Values in square brackets are 95% confidence intervals.

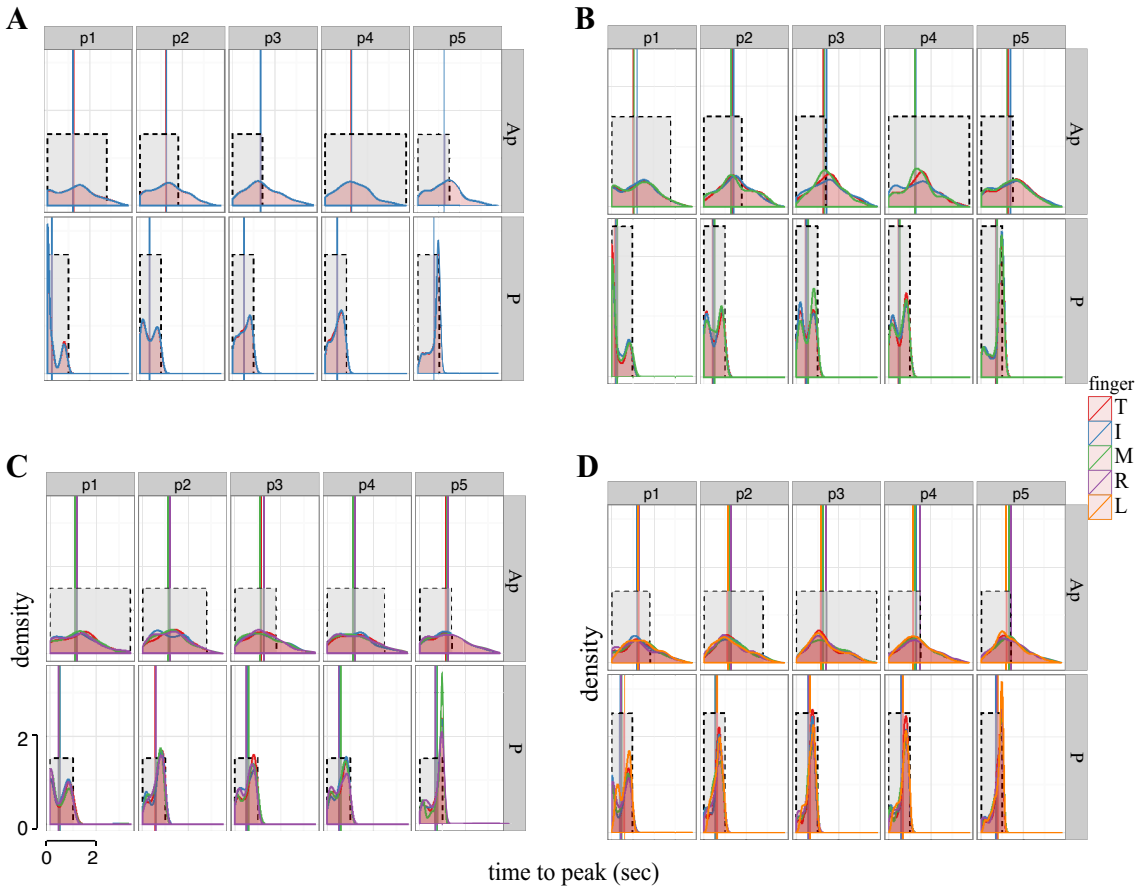

Fig. 6. Distribution of time to peak of digit normal forces across different trials and participants. Gray boxes represent the duration of external perturbations (p1–p5). Vertical lines represent the mean time to peak for each perturbation (LMM estimates). *A*: 2 digits. *B*: 3 digits. *C*: 4 digits. *D*: 5 digits. Ap denotes aperiodic trials (*top*) and P denotes periodic trials (*bottom*) in *A–D*.

shows the distributions of time to peak of normal force for the different digits, the perturbation number, and the perturbation frequency conditions. The distribution of the different digits was nearly indistinguishable in Fig. 6 (data detailed in Table 1). Accordingly, the difference in time to peak was not statistically significant between fingers [LR test; 2 digits: $\chi^2_{(1)} = 0.002$, $P = 0.96$; 3 digits: $\chi^2_{(2)} = 1.04$, $P = 0.56$; 4 digits: $\chi^2_{(3)} = 4.6$, $P = 0.2$; 5 digits: $\chi^2_{(4)} = 2.28$, $P = 0.68$]. Results of the repeated-measures ANOVA were in accordance with the LMM. The model could not find a significant difference in time to peak between the digits [2 digits: $F(1, 4) = 0.04$, $P = 0.84$; 3 digits: $F(2, 8) = 0.61$, $P = 0.57$; 4 digits: $F(3, 12) = 1.37$, $P = 0.30$; 5 digits: $F(4, 20) = 1.03$, $P = 0.42$]. These results suggest that time to peak was approximately synchronous between digits, which is consistent with a parallel control of the fingers in response to external perturbations. Additionally, we estimated the cross-correlation coefficients between different digits of the force profiles for each participant (5-digit condition only). As shown in Fig. 7, the average values of cross-correlation coefficients were rather high (0.73 ± 0.09, mean ± SD), supporting the hypothesis of a synergistic control of the five digits.

Next, we investigated the modulation in magnitude of grip force across perturbation number within each trial. To account for the nonlinearity of the effect (Fig. 8), we used a second-order polynomial of the form $\beta_1 P + \beta_2 P^2$, where P is the perturbation number and $\beta_{\{1,2\}}$ are the fixed-effect parameters as described in METHODS. We evaluated the significance of this nonlinear effect using the LR test. In all digit conditions, the effect of perturbation number was highly significant [2 digits: $\chi^2_{(2)} = 39.22$, $P < 0.01$; 3 digits: $\chi^2_{(2)} = 61.88$, $P < 0.01$; 4 digits: $\chi^2_{(2)} = 36.55$, $P < 0.01$; 5 digits: $\chi^2_{(2)} = 8.7$, $P < 0.01$]. The reaction force increased from the first (P1) to the fifth (P5) perturbation (Fig. 8), revealing a fast adaptation to external perturbations.

We next explored the question whether the learning pattern observed in digit force responses affected the stabilization of the TACO in response to the external torque within the first five perturbations. To this end, we averaged the data across trials, participants, and perturbation type for each digit condition, and we calculated the error of hand net as the difference between the participants' hand net torque and the required torque to counterbalance the external perturbation. Figure 9 shows the error of hand net torque for the aperiodic (Ap) and periodic (P) conditions during the five perturbations (perturbation number) per trial for each number of digits used. As expected, LMM revealed that the mean error in hand torque was higher for the Ap than the P condition for all types of grasp conditions (number of digits used). The difference in the net hand torque (T) between Ap and P conditions, $T_{Ap} - T_P$, was equal to 2.18 ± 0.24 (mean ± SE; 2 digits), 2.22 ± 0.27 (3 digits), 2.02 ± 0.26 (4 digits), and 1.05 ± 0.18 N·cm (5 digits).

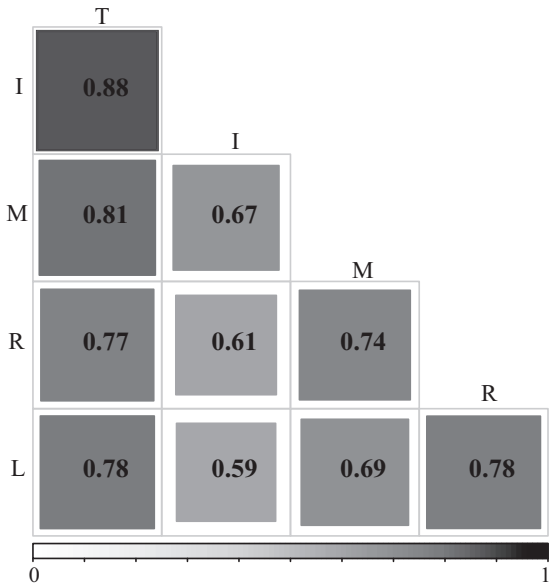

Fig. 7. Cross-correlation coefficients between digit normal force profiles (5-digit condition only). Values are averaged across perturbation types, trials, and participants.

As in the previous analysis, we used a second-order polynomial of the form $\beta_1 P + \beta_2 P^2$ to account for the nonlinearity of the effect of perturbation (Fig. 9). We evaluated the significance of the effect using the LR test. In all digit conditions, the nonlinear effect of perturbation was highly significant [2 digits: $\chi^2_{(2)} = 256.71$, $P < 0.01$; 3 digits: $\chi^2_{(2)}$ 275.73, $P < 0.01$; 4 digits:
$\chi^2_{(2)} = 528.75$, $P < 0.01$; 5 digits: $\chi^2_{(2)} = 446.80$, $P < 0.01$]. As shown in Fig. 9, the error in hand net torque drastically decreased across perturbations, revealing a fast adaptation to external perturbations. Moreover, according to LMM, there was an interaction effect between the number of perturbations and perturbation frequency in error of hand net torque as indicated by the LR test [2 digits: $\chi^2_{(4)} = 14.16$, $P < 0.01$; 3 digits: $\chi^2_{(4)} = 10.38$, $P = 0.03$; 4 digits: $\chi^2_{(4)} = 13.82$, $P < 0.01$; 5 digits: $\chi^2_{(4)} = 16.77$, $P < 0.01$]. This result showed that learning to compensate for the external torque was faster in the periodic than in the aperiodic condition, especially when a five-digit grasp was used (cf. Fig. 9).

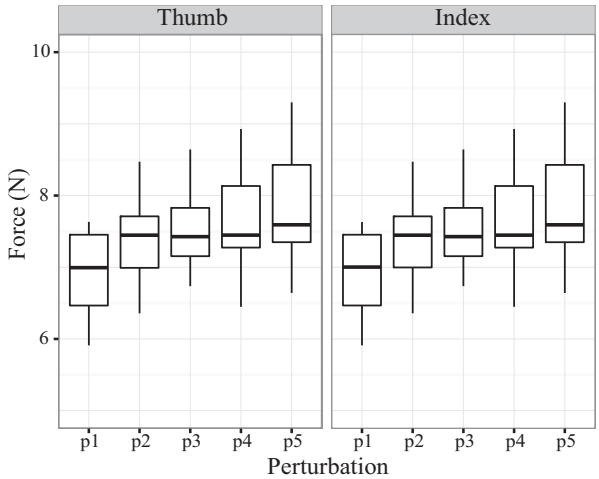

Fig. 8. Boxplot of the distribution of thumb and index normal forces in 5 perturbations (2-digit condition). Data are pooled across participants and trials.

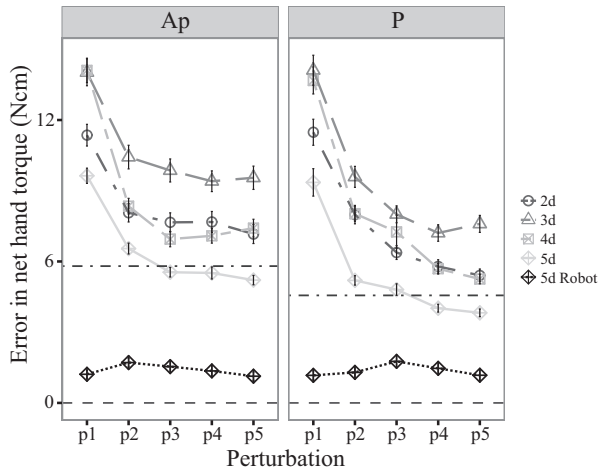

Fig. 9. Average error in hand net torque in the human hand (2d–5d, 2- to 5-digit conditions) and robot hand (Shadow Dexterous Hand). Data are averaged across participants and perturbation types with aperiodic (Ap; *left*) and periodic frequency (P; *right*). Horizontal dashed lines represent LMM estimates excluding p1 values in 5-digit condition. Error bars represent the SE of the model estimate.

Because of the different length of the lever arm produced by the external torques T_y and T_z (e.g., Fig. 4*C*) on each digit, we may expect a modulation of the peak reaction force between digits as a function of the direction of torques (clockwise and counterclockwise). Accordingly, Fig. 10, *B* and *C*, shows a clear trend as the normal force in the outer digits is modulated depending on the direction of the torque (compare for instance, Fig. 10*B*, torque counterclockwise, and Fig. 10*C*, torque clockwise). We applied a LMM to test for the interaction between T_y torque direction (T_y^{CCW}, T_y^{CW}) and digits (I, M, R, L) on the produced force. We found a significant a main effect of digits on the force responses [3 digits: $\chi^2_{(1)} = 6.93$, $P < 0.01$; 4 digits: $\chi^2_{(2)} = 28.52$, $P < 0.001$; 5 digits: $\chi^2_{(3)} = 413.54$, $P < 0.001$], but no effect of the perturbation direction [3 digits: $\chi^2_{(1)} = 2.49$, $P = 0.11$; 4 digits: $\chi^2_{(1)} = 0.48$, $P = 0.49$; 5 digits: $\chi^2_{(1)} = 1.67$, $P = 0.19$]. Crucially the interaction between direction and digits was statistically significant, confirming the hypothesis that the force modulation as a function of digit and direction [3 digits: $\chi^2_{(1)} = 12.69$, $P < 0.001$; 4 digits: $\chi^2_{(2)} = 43.98$, $P < 0.001$; 5 digits: $\chi^2_{(3)} = 74.14$, $P < 0.001$]. Additionally, we applied a LMM on peak digit normal force produced by the index and middle finger (we focused on these 2 fingers because both were present in 3-, 4-, and 5-digit conditions). The analysis revealed a significant effect of the perturbation type on the produced normal force [I: $\chi^2_{(4)} = 50.4$, $P < 0.001$; M: $\chi^2_{(4)} = 23.04$, $P < 0.001$].

In summary, in the rotational task (T_y^{CCW}, T_y^{CW}), the outer fingers produced a larger amount of force compared with the inner fingers (Fig. 10, *B* and *C*). The observed effect might be simply mechanical by nature. In other words, the farther the fingers are from the TACO's center, the higher the force exerted by the participants in the opposite direction to the external torque perturbation. To further test the validity of our interpretation, we conducted a control experiment using a robotic hand.

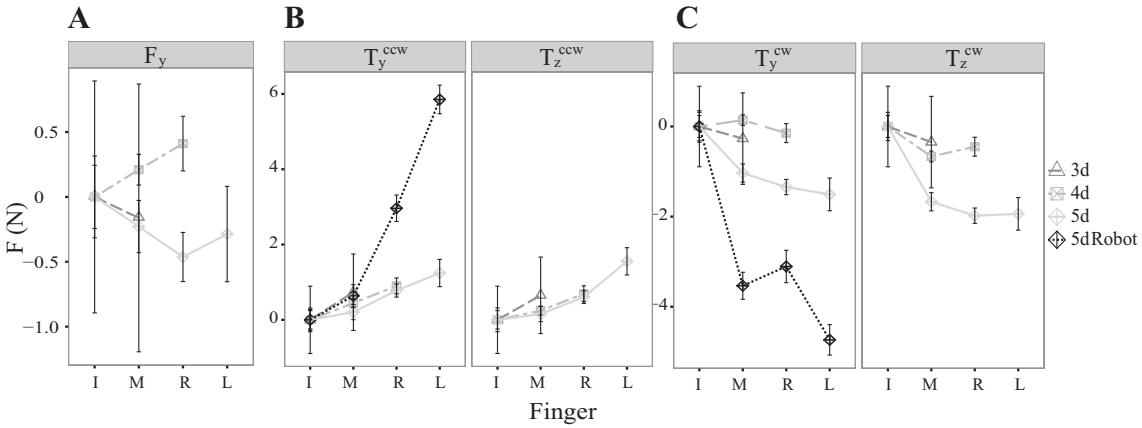

Fig. 10. Change in normal forces relative to the normal force exerted by the index finger. Mean values are given for the different digits in the human hand (3d–5d conditions) and robot hand (Shadow Dexterous Hand). Error bars represent SE. *A*: data for the perturbation F_y. *B*: data for perturbation torque T_y^{CCW} and T_z^{CCW}. *C*: data for perturbation torque T T_y^{CW} and T_z^{CW}.

Control experiment: robot hand. We considered two alternative motor strategies: either participants controlled the stiffness of all fingers jointly (grasping synergy), or they modulated the force of each finger independently in response to the given external perturbation. The former motor strategy is more parsimonious because it reduces the degrees of freedom of the system and is in accordance with the synchronous response of the different fingers. We evaluated whether the synergistic motor control was compatible with the asymmetry in normal force between outer and inner fingers observed in torque perturbation. To this end, we replicated the same experimental paradigm using the robotic hand (Shadow Dexterous Hand) programmed with a synergic control of fingers' stiffness. We tested conditions T_y^{CCW} and T_y^{CW} (5 digits; Fig. 11).

Because of the different friction coefficients between human and robot fingers, a larger normal force was required to obtain a stable grasp with the robot hand, which accounts for the larger reaction torque (Fig. 10). Errors in net hand torque, computed as the difference between the perturbation and the reaction torque, were smaller compared with those of human participants (Fig. 9) and were not significantly affected by perturbation type [$\chi^2_{(1)} = 2.21$, $P = 0.14$], perturbation frequency [$\chi^2_{(1)} = 0.02$, $P = 0.88$], and perturbations number [$\chi^2_{(4)} = 9.16$, $P = 0.06$]. Figure 10, *B* and *C* (dark rhombus with dotted line), shows mean normal force of each robot's finger, averaged across trials and the frequency condition (periodic and aperiodic). Similarly to findings in humans (gray lines), the index finger exerted a larger force relative to the other fingers in condition T_y^{CW} and the little and ring fingers exerted a relatively larger force in T_y^{CCW}. Because of the larger torque, this difference was larger compared with that of the human hand. This is also illustrated in Fig. 11 (single trial), showing that during external perturbation with T_y^{CCW}, the reaction force was higher for the little and ring fingers. Due to the controller that we implemented, this difference in force among fingers can only be ascribed to mechanical factors such as the length of the lever arm. Time to peak was not significantly different between the fingers [LR test; T, I, M, R, L: $\chi^2_{(4)} = 0.23$, $P = 0.99$] and between perturbation types (T_y^{CW}, T_y^{CCW}: $\chi^2_{(1)} = 3.83$, $P = 0.05$]. This was expected and indicates that digit times to peak force were synchronized between fingers.

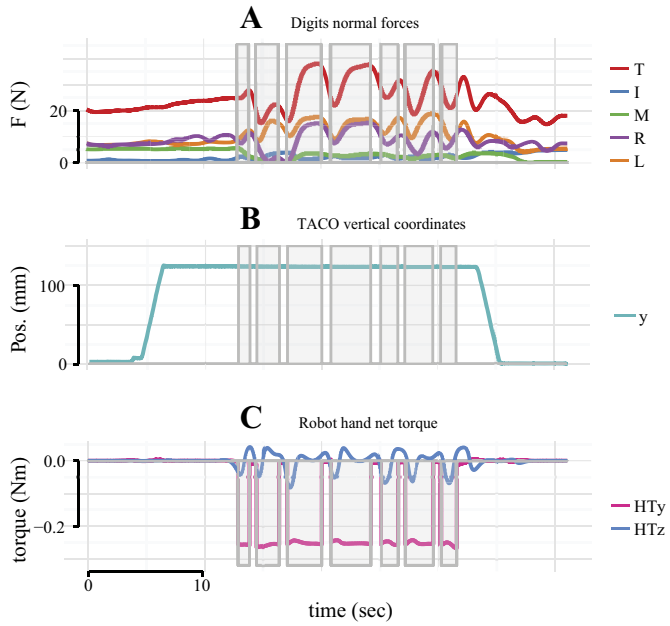

Fig. 11. Single trial data for the robot Shadow Dexterous Hand in T_y^{CCW} (areas boxed in gray represent another example of aperiodic intervals when external perturbations are active "on"). *A*: force profiles for each digit. *B*: TACO vertical coordinates along *y*-axis. *C*: robot hand net torques.

In summary, the asymmetry in the normal force between fingers that we observed in human grasp can be qualitatively reproduced by the robotic hand, where the only controlled variable was the global hand stiffness. The hand-stiffening strategy successfully compensated the external torque regardless of the external perturbation frequency and type. The differences between the robot and human hand data were the larger torques and forces exerted by the robotic hand, the absence of a learning trend observed between the earliest perturbations (P1 and P2) vs. the rest of the perturbations, and the lack of difference between periodic and aperiodic conditions. The grasp controller employed in the robot hand did not actively control the grasping forces of the individual fingers to counteract disturbances. Therefore, the difference in force among fingers was due to their locations on the TACO. The larger the lever arm is, the higher is the reactive finger force opposing the external torque.

DISCUSSION

Summary of results. In the current study, we evaluated the force response to external perturbations during multidigit grasping. The position of the fingers on the manipulandum was unconstrained, which is a methodological novelty with respect to previous studies. We found that the modulation of the force responses was almost synchronous across digits, in accordance with a synergistic control of the hand. Furthermore, participants were better able to stabilize the manipulandum in the periodic than aperiodic condition, thus suggesting a feedforward motor strategy when participants could predict the upcoming perturbations. This is consistent with previous studies showing that to reduce motor delays and to attain grasp stability, the CNS manifests feedforward properties based on an anticipatory control of force mediated by internal models (Budgeon et al. 2008; Johansson and Flanagan 2008). However, alternative mechanisms have been proposed, including controlling the muscle activation threshold, i.e., the muscle length at which motor neurons begin their recruitment (Latash et al. 2010; Pilon and Feldman 2006; Pilon et al. 2007). This feedforward, synergistic motor strategy was employed in the current experiment regardless of the type of external perturbation or the number of digits used in the grasping task. In a control experiment, we replicated the grasping task with a robotic hand that employed a simple stiffness controller, and we observed a force distribution that was qualitatively similar to that obtained from experiments with humans. The main difference between human and robot grasp was that human participants quickly adapted their grip force within the first few perturbations to successfully compensate for external perturbations.

Idiosyncratic hand posture. Our experimental setup allowed participants to freely choose the placement of their fingers on the object while grasping. This revealed large variability between participants in the initial digit placement. Friedman and Flash (2007) also observed a large amount of variability in finger placement on common objects with the use of five-digit grasps. Although the task is stereotypical, initial digit position seems to be highly preserved across stimulus repetitions for individual participants. This has been confirmed by *k*-means clustering analysis and ANOVA and can be explained by idiosyncratic grasping strategies.

Control of grip force. The time to peak normal force was nearly synchronous across all digits engaged in grasping within a single perturbation (Figs. 6 and 7 and Table 1), suggesting that digit normal forces were controlled as a unit within a single perturbation. Similarly, synchronous force changes were found when the fifth finger was added or removed during the hold phase of the grasping task (Budgeon et al. 2008) and during tripod grasps (Budgeon et al. 2008; Winges et al. 2007). In the current task, a change in reaction force was indistinguishable from a change in finger stiffness opposing the perturbation. For simplicity, we assumed that the change in reaction force measured with the apparatus was due to a change in finger stiffness (or pseudo-stiffness; see below), because the type of the force perturbation varied unpredictably from trial to trial. A motor strategy based on the control of hand stiffness would be in accordance with previous literature on hand grasping (Milner and Franklin 1998; Winges et al. 2007). We recognize, however, that because of possible changes in muscle length due to involuntary contractions and attenuation of reflex responses following repeated perturbations (Rothwell et al. 1986; Turpin et al. 2016), the term pseudo-stiffness would be more appropriate. Finally, it is important to remark that the aim of the experiment was to evaluate whether participants controlled different digits independently or in a synergistic fashion, and not whether they used a stiffness or force control. The hypothesis of a synergistic motor strategy was confirmed by the results of the control experiment with the Shadow Dexterous Hand, which employed a single controller for the whole hand without considering force modulation at each individual finger. Force profile was qualitatively similar between the robot and human participants.

Learning within a trial. The feedforward stiffening strategy led to stable grasp that optimized the error in the hand net torque across perturbations, indicating that the hand-stiffening strategy was resistive to external perturbations (Hasan 2005). Previous studies showed that human adaptation to the perturbation is performed on a trial-to-trial basis by feeding the error of previous trial into the feedforward controller of the current trial (Lukos et al. 2013; Shadmehr et al. 2010). In our results, digit normal force increased from the first perturbation to subsequent ones with the result that the error in net hand torque dropped (Figs. 8 and 9). This suggests that digit normal forces are adapted across consecutive perturbations during the holding phase such that grip force (whole hand stiffening) is gradually increased from one perturbation to the next. Such a simple strategy seems sufficient to successfully counterbalance disturbances on the TACO and consequently to reduce the error in hand net torque caused by predictable and unpredictable perturbations. A similar observation was made with tripod grasps conducted in a study by Winges et al. (2007), in which they suggested that the neuromuscular control system compensated for predictable and unpredictable object mechanical properties by pursuing inherent global stiffness of the hand through co-contraction and modulation of hand muscle activity. The only difference between predictable and unpredictable conditions was the error in hand net torque that was reduced faster in the predictable condition compared with the unpredictable one, especially after the first perturbation (the interaction effect). This latter result can be explained by the work of Aimola et al. (2014) that showed the onset of muscle response took longer in the unpredictable than in the predictable condition. They suggest that precise prediction of the perturbation sequence improves muscle responses, thus shortening the latency of muscle activity in relation to the mechanical perturbation.

Concerning the normal forces of individual digits, we observed a relatively higher force response in the outer fingers. This effect can be explained solely as a mechanical consequence of the full hand stiffening and the outer fingers' longer moment arm: the farther the finger from the center of the TACO, the higher the normal force in a torque perturbation. This result was confirmed in the control experiment using the Shadow Dexterous Hand, which employed a simple stiffness controller of the entire robotic hand. In this experiment we observed a similar force trend between digits position (outer vs. inner) for a five-digit grasp (Fig. 10).

The stiffening strategy was observed regardless of the external perturbations and the number of digits used in the task. Therefore, on the basis of our results, the modulation of digit

normal forces may be a "configuration" rather than a "specialization" outcome (Wu et al. 2012; Zatsiorsky et al. 2002). In the domain of digit normal force, it has been reported that two force synergies (i.e., two principal components) accounted for more than 90% of the finger force variance in constrained and unconstrained grasping (Naceri et al. 2014; Zatsiorsky and Latash 2004). The robot hand has only the first synergy of full hand closure when its stiffness controller is engaged. This might suggest that the second synergy found in human studies is of mechanical, rather than neural, origin and is caused by the fingers' moment arm and digit-object interaction forces caused by the external perturbation.

Despite the high variability in initial placement of digits and the number of digits used in the task, the synchronous digits stiffening strategy persisted throughout all conditions of the experiment and for all participants. A contribution from biomechanical constraints acting on finger muscles (Santello et al. 2013) could also account for the strategy adopted by participants. Different hand postures led to different grasp stiffness (Friedman and Flash 2007) and different grip force (Naceri et al. 2014), but each satisfied a stable grasp because of the canceling of the applied perturbation forces (equilibrium). It has been shown that arbitrary net force and/or torques produced by force closure of a robotic hand (SoftHand) satisfy a stable grasp in the absence of friction forces (Bicchi et al. 2011). In addition, the latter work showed that with one synergy in the kinematic domain, the robotic hand was able to grasp a large variety of daily objects. With this work, we have shown that one force synergy is sufficient to resist different types of external perturbations while achieving a stable grasp.

In conclusion, participants substantially varied in their initial placements of their fingers on the TACO. Once they grasped and lifted the object using the required grip, the magnitude of digit normal force corrective responses was controlled in a feedforward manner within single perturbations. However, hand net torque was optimized across perturbations by increasing the grip force in the perturbations following the first disturbance, which indicates that participants gradually adapted their feedforward whole hand stiffening across perturbations. The synchronous increase of digit normal forces was achieved by all digits regardless of the external perturbation and the number of digits involved in the task. This suggests that in a simple grasping and holding task, the CNS adopts a stiffening strategy that compensates for the task uncertainty associated with unpredictable external perturbations and with the variability in required grip force. This finding underscores the flexibility and independence of high-level motor processing from low-level motor execution by end effectors (Fu et al. 2011).

ACKNOWLEDGMENTS

We thank Edin Benoni for useful comments and discussion. We also thank Dr. Guillaume Walck for technical support in the control experiment and Dr. Jonathan Maycock for scientific comments and English proofreading of the manuscript and Florian Lier for providing us the avatar model of figure 1a which is part of MORSE open source project.

GRANTS

This research was partially supported by National Science Foundation Collaborative Research Grant BCS-1455866 (to M. Santello), European Commission IP Grant 601165 "WEARable HAPtics," and Deutsche Forschungsgemeinschaft Center of Excellence EXC 277: Cognitive Interaction Technology (CITEC).

DISCLOSURES

No conflicts of interest, financial or otherwise, are declared by the authors.

AUTHOR CONTRIBUTIONS

A.N. and R.H. performed experiments; A.N., A.M., and R.H. analyzed data; A.N., A.M., M.S., and M.O.E. interpreted results of experiments; A.N. prepared figures; A.N. drafted manuscript; A.N., A.M., R.H., H.R., M.S., and M.O.E. edited and revised manuscript; A.N., A.M., R.H., H.R., M.S., and M.O.E. approved final version of manuscript.

REFERENCES

Aimola E, Valle MS, Casabona A. Effects of predictability of load magnitude on the response of the flexor digitorum superficialis to a sudden fingers extension. *PLoS One* 9: e109067, 2014. doi:10.1371/journal.pone.0109067.

Bates D, Mächler M, Bolker B, Walker S. Fitting linear mixed-effects models using lme4. *J Stat Softw* 67: 1–48, 2015. doi:10.18637/jss.v067.i01.

Baud-Bovy G, Soechting JF. Factors influencing variability in load forces in a tripod grasp. *Exp Brain Res* 143: 57–66, 2002. doi:10.1007/s00221-001-0966-8.

Bicchi A, Gabiccini M, Santello M. Modelling natural and artificial hands with synergies. *Philos Trans R Soc Lond B Biol Sci* 366: 3153–3161, 2011. doi:10.1098/rstb.2011.0152.

Bolker BM, Brooks ME, Clark CJ, Geange SW, Poulsen JR, Stevens MH, White JS. Generalized linear mixed models: a practical guide for ecology and evolution. *Trends Ecol Evol* 24: 127–135, 2009. doi:10.1016/j.tree.2008.10.008.

Budgeon MK, Latash ML, Zatsiorsky VM. Digit force adjustments during finger addition/removal in multi-digit prehension. *Exp Brain Res* 189: 345–359, 2008. doi:10.1007/s00221-008-1430-9.

Friedman J, Flash T. Task-dependent selection of grasp kinematics and stiffness in human object manipulation. *Cortex* 43: 444–460, 2007. doi:10.1016/S0010-9452(08)70469-6.

Fu Q, Hasan Z, Santello M. Transfer of learned manipulation following changes in degrees of freedom. *J Neurosci* 31: 13576–13584, 2011. doi:10.1523/JNEUROSCI.1143-11.2011.

Fu Q, Zhang W, Santello M. Anticipatory planning and control of grasp positions and forces for dexterous two-digit manipulation. *J Neurosci* 30: 9117–9126, 2010. doi:10.1523/JNEUROSCI.4159-09.2010.

Hasan Z. The human motor control system's response to mechanical perturbation: should it, can it, and does it ensure stability? *J Mot Behav* 37: 484–493, 2005. doi:10.3200/JMBR.37.6.484-493.

Johansson RS, Flanagan JR. Tactile sensory control of object manipulation in humans. In: *The Senses: A Comprehensive Reference*, edited by Basbaum AI, Kaneko A, Shepherd GM, and Westheimer G. San Diego, CA: Academic, 2008, p. 67–86.

Johansson RS, Westling G. Roles of glabrous skin receptors and sensorimotor memory in automatic control of precision grip when lifting rougher or more slippery objects. *Exp Brain Res* 56: 550–564, 1984. doi:10.1007/BF00237997.

Latash ML. Movements that are both variable and optimal. *J Hum Kinet* 34: 5–13, 2012. doi:10.2478/v10078-012-0058-9.

Latash ML, Friedman J, Kim SW, Feldman AG, Zatsiorsky VM. Prehension synergies and control with referent hand configurations. *Exp Brain Res* 202: 213–229, 2010. doi:10.1007/s00221-009-2128-3.

Lukos J, Ansuini C, Santello M. Choice of contact points during multidigit grasping: effect of predictability of object center of mass location. *J Neurosci* 27: 3894–3903, 2007. doi:10.1523/JNEUROSCI.4693-06.2007.

Lukos JR, Ansuini C, Santello M. Anticipatory control of grasping: independence of sensorimotor memories for kinematics and kinetics. *J Neurosci* 28: 12765–12774, 2008. doi:10.1523/JNEUROSCI.4335-08.2008.

Lukos JR, Choi JY, Santello M. Grasping uncertainty: effects of sensorimotor memories on high-level planning of dexterous manipulation. *J Neurophysiol* 109: 2937–2946, 2013. doi:10.1152/jn.00060.2013.

Milner TE, Franklin DW. Characterization of multijoint finger stiffness: dependence on finger posture and force direction. *IEEE Trans Biomed Eng* 45: 1363–1375, 1998. doi:10.1109/10.725333.

Moscatelli A, Mezzetti M, Lacquaniti F. Modeling psychophysical data at the population-level: the generalized linear mixed model. *J Vis* 12: 1–17, 2012. doi:10.1167/12.11.26.

Naceri A, Moscatelli A, Santello M, Ernst MO. Coordination of multi-digit positions and forces during unconstrained grasping in response to object perturbations. 2014 IEEE Haptics Symposium (HAPTICS), Houston, TX, 2014, p. 35–40. doi:10.1109/HAPTICS.2014.6775430.

Pilon JF, De Serres SJ, Feldman AG. Threshold position control of arm movement with anticipatory increase in grip force. *Exp Brain Res* 181: 49–67, 2007. doi:10.1007/s00221-007-0901-8.

Pilon J-F, Feldman AG. Threshold control of motor actions prevents destabilizing effects of proprioceptive delays. *Exp Brain Res* 174: 229–239, 2006. doi:10.1007/s00221-006-0445-3.

Pinheiro J, Bates D. *Mixed-Effects Models in S and S-PLUS*. New York: Springer, 2000.

Rothling F, Frank R, Robert H, Steil JJ, Helge R. Platform portable anthropomorphic grasping with the Bielefeld 20-DOF shadow and 9-DOF TUM hand. In: 2007 IEEE/RSJ International Conference on Intelligent Robots and Systems, San Diego, CA, 2007, p. 2951–2965. doi:10.1109/IROS.2007.4398963.

Rothwell JC, Day BL, Berardelli A, Marsden CD. Habituation and conditioning of the human long latency stretch reflex. *Exp Brain Res* 63: 197–204, 1986. doi:10.1007/BF00235664.

Russo M, D'Andola M, Portone A, Lacquaniti F, d'Avella A. Dimensionality of joint torques and muscle patterns for reaching. *Front Comput Neurosci* 8: 24, 2014. doi:10.3389/fncom.2014.00024.

Santello M, Baud-Bovy G, Jörntell H. Neural bases of hand synergies. *Front Comput Neurosci* 7: 23, 2013. doi:10.3389/fncom.2013.00023.

Santello M, Bianchi M, Gabiccini M, Ricciardi E, Salvietti G, Prattichizzo D, Ernst M, Moscatelli A, Jörntell H, Kappers AM, Kyriakopoulos K, Albu-Schäffer A, Castellini C, Bicchi A. Hand synergies: integration of robotics and neuroscience for understanding the control of biological and artificial hands. *Phys Life Rev* 17: 1–23, 2016. doi:10.1016/j.plrev.2016.02.001.

Santello M, Flanders M, Soechting JF. Postural hand synergies for tool use. *J Neurosci* 18: 10105–10115, 1998.

Schurmann C, Kõiva R, Haschke R, Ritter H. A modular high-speed tactile sensor for human manipulation research. In: IEEE World Haptics Conference, Istanbul, 2011, p. 339–344. doi:10.1109/WHC.2011.5945509.

Schurmann C, Kõiva R, Haschke R, Ritter H. Analysis of human grasping under task anticipation using a tactile book. In: 2012 12th IEEE-RAS International Conference on Humanoid Robots (Humanoids 2012), Osaka, Japan, 2012, p. 773–778. doi:10.1109/HUMANOIDS.2012.6651607.

Shadmehr R, Smith MA, Krakauer JW. Error correction, sensory prediction, and adaptation in motor control. *Annu Rev Neurosci* 33: 89–108, 2010. doi:10.1146/annurev-neuro-060909-153135.

Turpin NA, Levin MF, Feldman AG. Implicit learning and generalization of stretch response modulation in humans. *J Neurophysiol* 115: 3186–3194, 2016. doi:10.1152/jn.01143.2015.

Westling G, Johansson RS. Factors influencing the force control during precision grip. *Exp Brain Res* 53: 277–284, 1984. doi:10.1007/BF00238156.

Winges SA, Soechting JF, Flanders M. Multidigit control of contact forces during transport of handheld objects. *J Neurophysiol* 98: 851–860, 2007. doi:10.1152/jn.00267.2007.

Wu Y-H, Zatsiorsky VM, Latash ML. Multi-digit coordination during lifting a horizontally oriented object: synergies control with referent configurations. *Exp Brain Res* 222: 277–290, 2012. doi:10.1007/s00221-012-3215-4.

Zatsiorsky VM, Gregory RW, Latash ML. Force and torque production in static multifinger prehension: biomechanics and control. I. Biomechanics. *Biol Cybern* 87: 50–57, 2002. doi:10.1007/s00422-002-0321-6.

Zatsiorsky VM, Latash ML. Multifinger prehension: an overview. *J Mot Behav* 40: 446–476, 2008. doi:10.3200/JMBR.40.5.446-476.

Zatsiorsky VM, Latash ML. Prehension synergies. *Exerc Sport Sci Rev* 32: 75–80, 2004. doi:10.1097/00003677-200404000-00007.